Single-stage PV System With Multi-Objective Predictive Control Approach

Simone Vanti
Dep. of Management and Engineering
Uni. of Padua
Italy 35122 Padova PD
Email:simone.vanti@studenti.unipd.it

Prabhat Ranjan Bana
Dep. of Electric Power Engineering
Norwegian Uni. of Science and Tech.
Trondheim, Norway
Email: prabhat.r.bana@ntnu.no

Mohammad Amin
Dep. of Electric Power Engineering
Norwegian Uni. of Science and Tech.
Trondheim, Norway
Email: mohammad.amin@ntnu.no

***Abstract*—Model predictive control (MPC) as a current controller has gained attention in a grid-connected power electronic converter system. The multi-objective predictive control is in greater demand when the photovoltaic (PV) sources are integrated with the utility grid since the inverter alone must ensure all of the control objectives such as grid current following, constant power factor operation and accurate maximum power point tracking (MPPT) performance. In this regard, this paper aims to implement the multi-objective Finite Set Control (FCS) - MPC for a single-stage grid-connected PV system considering the two-stage system is less cost-effective, more loss and less reliable. Moreover, the classical MPPT fails to extract the maximum power under fluctuating and shaded environmental condition. Therefore, an improved MPPT algorithm is proposed in this work which is again combined with the multi-objective FCS-MPC to ensure the extraction of the maximum power from the PV and good transient performance of the grid-side voltage and current. Two different approaches for the dc-voltage tracking are compared, one is implemented with an outer-loop proportional integral controller and the second one is implemented directly in the MPC objective function. The output findings clearly show the single-stage PV system with the proposed control can ensure a fast and accurate maximum power tracking and maintenance of stable output signal throughout all the transient conditions.**

***Index Terms*—Model predictive control (MPC), Maximum power point tracking (MPPT), Solar photovoltaic (PV) generation, Voltage source converter (VSC).**

I. Introduction

Considering all the several renewable energy options available, solar energy tops the list. Solar energy is first converted into dc-power with the help of a PV array and then converted into ac-power through an inverter and fed to the grid. Two typical configurations of a grid-tied PV system are the single-stage conversion and two stages configuration [14].

The standard two-stage grid-connected PV system is presented in [15]. The merit of two stages topology lies in the convenience of designing its control scheme but in trade-off with cost and power loss. The system consists of a solar panel, a dc-dc boost converter and an inverter. The implementation of the boost convert ensures the independence of panels dc-voltage v_{pv} and the inverter dc-voltage v_{dc}. Hence the v_{dc} is maintained stable by an external voltage loop control of the inverter, the control of the output variables are facilitated and even a low current total harmonic distortion (THD) is easier to obtain. Even though this well known solution has been in existence for a while, due to lower efficiency along with higher costs, bigger size and low reliability of the two-stage configurations, single-stage PV power process are becoming an important topic in the last decade.

The single-stage configuration as shown in Fig. 1 uses only one power converter, which leads to higher efficiency and lowers costs compared with the two-stage topology. A three-level neutral point clamped (3L NPC) inverter is considered in Fig.1 although other inverter structures from two-level to multilevel can also be employed. Several different implementations of single-stage grid-connected PV systems are already proposed in many literatures [10], [11] where pulse width-modulator (PWM) control and using a fuzzy logic controller are presented respectively.

In the literature, various types of classical and modern control schemes have been studied and proposed in order to improve the performance of the voltage source converter (VSC), such as cascaded linear regulators and a PWM [6], [8], linear quadratic controller (LQR)[12]. These control schemes, in a way or another, are characterized by several limitations.

In clear contrast to linear control, FCS-MPC is based on a fundamentally different principle. Instead of designing an independent loop for every controlled variable and then cascading them together, it uses a discrete model of the VSC with associated filter to predict its future behavior for all possible control inputs and consequently applying the optimal switching signals based on the minimization of a pre-defined cost function, which represents the desired behavior of the system [2], [1]. Considering a wide range of power electronics application, MPC has been implemented in many literatures [9], [13] however, the application of MPC in the single-stage PV system is still new to achieve the aforesaid benefits.

The main contribution of this paper is to control the single-stage grid-connected PV system with the combination of FCS-MPC and an improved MPPT control method. The single-stage PV system with the proposed control is capable of following the MPP even under partially shaded conditions. Partially shaded condition depicts multiple peaks in the power-voltage $(p-v)$ curve and classic MPPT algorithms [7] are unable to track the MPP. Therefore, an improved MPPT algorithm is proposed in this work to extract the maximum power from the single-stage application. Moreover, a 100 kW PV system

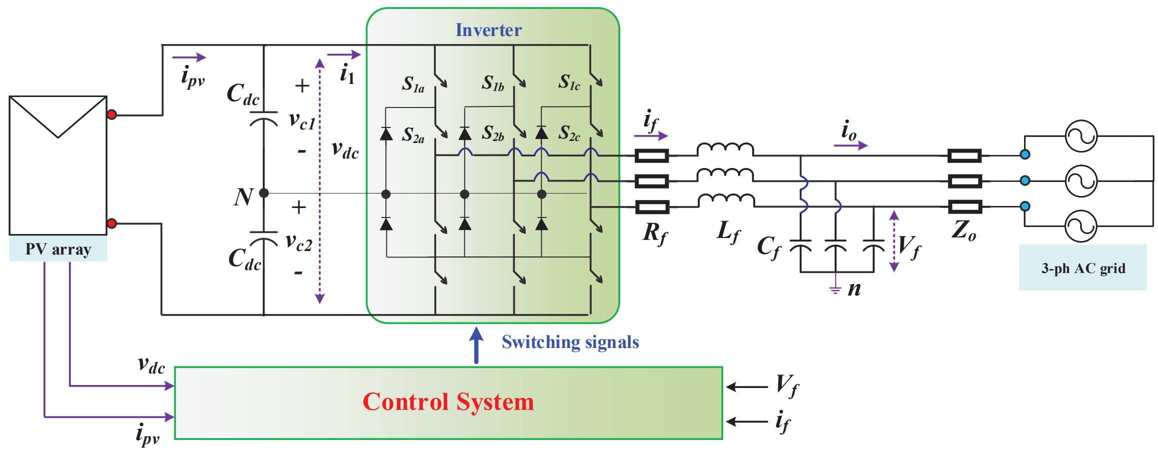

Fig. 1. Schematic of single-stage grid-tied PV system with the proposed control system.

connected to the 25 kV grid via a three-phase 3L NPC VSC is considered in this work to validate the workability of the proposed control algorithm.

The rest of the paper is organized in the following. Section II presents the analytical modeling and control of the system. Section III presents the modeling of the improved MPPT technique. Simulation results are presented in section IV followed by the concluding remarks in section V.

II. Analytical Modeling of the VSC and it's Control System

System modeling is an essential part before designing any control schemes. The following section includes the detailed single-stage PV system design and MPC control application.

A. Implementation of the FCS-MPC with the PV VSC

The grid-connection of the dc source is achieved with an NPC inverter and LCL filter as illustrated in Fig.1. Therefore, the system model of the system consists of two parts: the dynamics of the line currents and the dynamics of the voltages across the two dc-bus capacitors. This model is used to perform the predictive control of the converter where the main control objectives need to be achieved: 1) balanced and symmetrical injected line currents, 2) balanced dc-link capacitor voltages 3) dc-voltage tracking.

The respective VSC will be modeled here using a stationary $\alpha\beta$ orthogonal reference frame. To that end, all generic three-phase voltages v and currents i, given in $a-b-c$ can be transformed into corresponding $\alpha\beta$ frame by applying an amplitude invariant Clarke transformation [2]

B. Dynamics of the lines currents

The voltage vectors, $v_{\alpha\beta}$ in the complex domain are presented for 27-switch configuration patterns as presented in [5]

The common mode voltage, v_{nN} can be deducted from Fig.1 in order to obtain the phase voltage expression, $\bar{v}_{in}$ given by:

$$\bar{v}_{in} = \bar{v}_{iN} - v_{nN}. \tag{1}$$

With reference to the power circuit of Fig.1 and applying Kirchoof laws, the inverter's voltages in the $\alpha\beta$ reference frame can be expressed as:

$$\bar{v}_{in} = R_f \bar{i}_f + L_f \frac{d\bar{i}_f}{dt} - \bar{v}_f \tag{2}$$

where the current dynamic can be extrapolated as follow

$$L_f \frac{d\bar{i}_f}{dt} = \bar{v}_{in} - \bar{v}_f - R_L \bar{i}_f. \tag{3}$$

The MPC algorithms are usually implemented in digital hardware platforms like DSPs or field-programmable gate arrays (FPGAs). For this reason, the prediction model of the system needs to be discretized. Using the Forward Euler approximation [2] as

$$\frac{d\bar{i}_{\alpha\beta}}{dt} \approx \frac{\bar{i}_{\alpha\beta}(k+1) - \bar{i}_{\alpha\beta}(k)}{T_s}. \tag{4}$$

where T_s is the sampling period. The line current dynamics can be expressed in discrete form as

$$\bar{i}_f(k+1) = (1 - \frac{R_L T_s}{L})\bar{i}_f(k) + \frac{T_s}{L}[\bar{v}_{in}(k) - \bar{v}_f(k)] \tag{5}$$

which estimates the current at the next sample $(k+1)$.

C. Dynamics of the dc-bus voltage and cost function evaluation

The voltage prediction of each capacitance on the dc side at the next sample time can be given by

$$v_{c1}(k+1) = v_{c1}(k) + \frac{(i_{pv}(k) - i_p(k))\,T_s}{C_{dc}} + \frac{i_0(k)T_s}{2C_{dc}} \tag{6}$$

$$v_{c2}(k+1) = v_{c2}(k) + \frac{(i_{pv}(k) + i_n(k))\,T_s}{C_{dc}} - \frac{i_0(k)T_s}{2C_{dc}} \tag{7}$$

where

$$i_0(k) = \overline{S}_0 \bar{i}_{abc} \text{ with } S_{x0} = \begin{cases} 1 & if\, S_x = 0 \\ 0 & \text{otherwise} \end{cases} ; x = \{a,b,c\} \tag{8}$$

$$i_p(k) = \overline{S}_p \bar{i}_{abc} \text{ with } S_{xp} = \begin{cases} 1 & if\, S_x = 1 \\ 0 & \text{otherwise} \end{cases} ; x = \{a,b,c\} \tag{9}$$

$$i_n(k) = \overline{S}_n \bar{i}_{abc} \text{ with } S_{xn} = \begin{cases} 1 & if\, S_x = -1 \\ 0 & \text{otherwise} \end{cases} ; x = \{a,b,c\}. \tag{10}$$

To perform an accurate tracking of the references currents, achieve balanced voltages across the dc-bus and tracking dc-voltage reference from the MPPT algorithm, the cost function must contain a term of each objective. Furthermore, in order to limit the switching frequency and avoid inrush current, two more terms are added in the cost function evaluation. The final cost function consider in the proposed system is described as follow

$$g = g_c + \gamma_b g_{bal} + \gamma_v g_{pv} + \gamma_u sw^2 + h_{lim} \tag{11}$$

where

$$\begin{aligned} g_c &= (i^*_{f\alpha} - i_{f\alpha})^2 + (i^*_{f\beta} - i_{f\beta})^2 \\ g_{bal} &= (v_{c1}(k+1) - v_{c2}(k+1))^2 \\ g_{pv} &= (v_{dc-ref} - (v_{c1}(k+1) + v_{c2}(k+1))^2 \end{aligned}$$

γ_b and γ_v are the voltage balance and the dc-voltage tracking weighting factor respectively. The factor sw^2 is used to penalize the switching effort which is again controlled by the weight factor γ_u; h_{lim} is the additional current constraint factor whose value is infinite if the current is higher than the physical inrush current limit of the inverter, i_{lim} else it is considered as zero.

The reference current is obtained as

$$i^*_f = \frac{2}{3} T_{dq/\alpha\beta} \cdot P_{set} \cdot \eta \cdot \frac{1}{V_d} \tag{12}$$

where V_d is the real component of the output voltage on the rotating reference frame, η the efficiency of the inverter which can be set to 0.95, P_{set} is the instantaneous power from the PV panels as $P_{set} = v_{dc} i_{pv}$ and $T_{dq/\alpha\beta}$ is the Park matrix transformation as given by

$$T_{dq/\alpha\beta} = \begin{bmatrix} \cos(\theta) & -\sin(\theta) \\ \sin(\theta) & \cos(\theta) \end{bmatrix} \tag{13}$$

where θ is the position of the voltage vector $v_{\alpha\beta}$ estimated with a Phase-locked-loop (PLL).

The schematic of the control systems for the grid-connected single-stage PV system is presented in Fig.2 where a single step prediction horizon is implemented. The MPPT algorithm presented in next section generates the dc-voltage reference, v_{dc-ref}.

D. Alternative dc-voltage tracking

The superiority of the proposed solution is verified with a comparison with a PI&MPC control solution in which the dc-voltage tracking is handled by an external PI controller. The entire schematic block with the proposed PI&MPC control is depicted in Fig.3 where the ΔP is obtained from the v_{pv} multiplied to the Δi extrapolated from the PI control. The ΔP is added to the Feed-Forward power factor P_{ff} obtained like $v_{dc-ref} \cdot i_{pv}$ in order to achieve the reference power value P_{set}. A similar approach is proposed even in [3]. The contribution of this paper is the integration of the dc-voltage control proposed in [3] with the FCS-MPC control described as before. It is worth mentioning, the dc-voltage control is not managed by the FCS-MPC and therefore the cost weighting factor given in (11) can be set to 0.

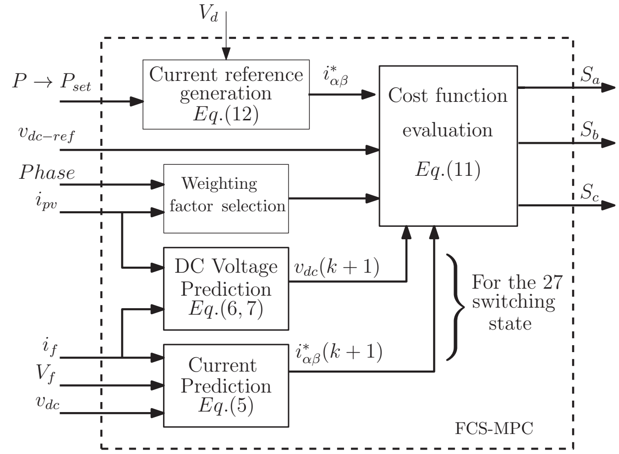

Fig. 2. The proposed FCS-MPC control system.

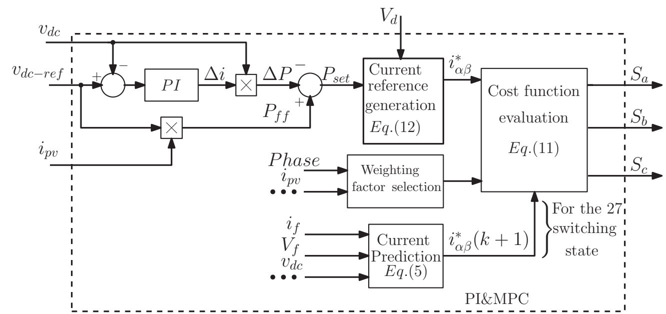

Fig. 3. The PI&MPC control system.

III. MPPT ALGORITHM

The traditional MPPT algorithms are not able to operate in the single-stage PV application as they are usually implemented in the middle boost converter which has been removed. Under uniform irradiance, even the well know algorithm P&O and Incremental conductance are able to find the maximum power point (MPP). Under partially shaded condition, the research of the global maximum power point (GMPP) become more complicated or even impossible for those algorithms previously cited as multi MPP peaks appear as described in Fig.4 wherein the parenthesis it's reported the value of the irradiance of each modules starting from the upper one. The classical algorithm could fall in one of the local MPP or find the GMPP too slow as the GMPP could be every whereas

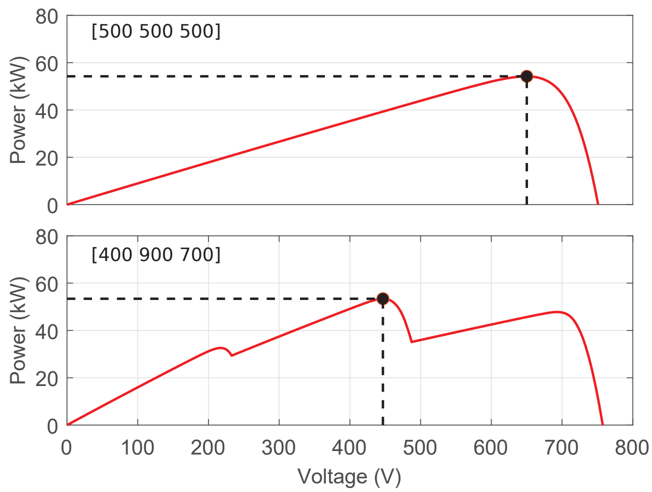

Fig. 4. Effects of shading condition on the $p-v$ characteristic: a) uniform irradiance equal to $500\mathrm{W/m^2}$ b) irradiance equal to $[400\,900\,700]$.

TABLE I
VSC AND SIMULATION PARAMETERS

Parameter	Description	Value
P_{PV}	maximum power	100kW
T_{sd}	Simulink time discretization	$1*10^{-6}$s
T_s	Sample Time	$1*10^{-4}$s
T_{MPPT}	Sample Time of MPPT algh.	$1*10^{-3}$s
V_{grid}	Utility Grid	25kV
L_f	Filter inductance	0.7mH
C_f	Capacitor bank	10kvar
R_L	Resistive filter components	0.00377Ω
C_{dc}	Capacitance on DC side	$3mF$
η	Inverter efficiency	0.95

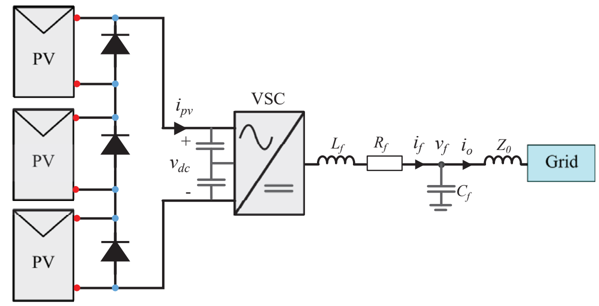

Fig. 5. System to test the partially shaded condition.

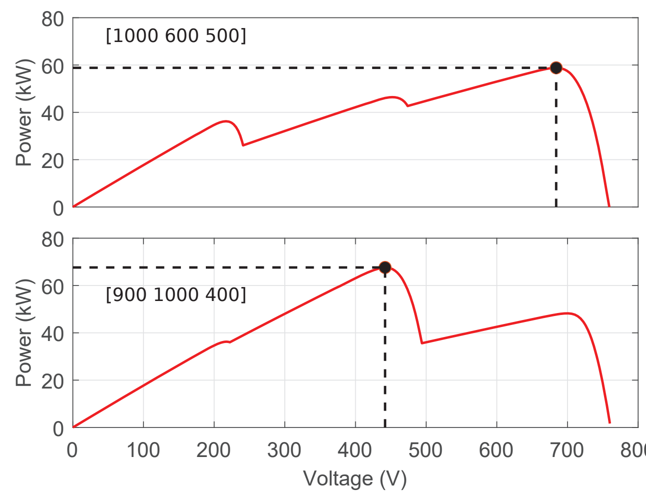

Fig. 6. Ideal $p-v$ curve with irradiance set equal to $[1000 \cdot 600 \cdot 500]$ and $[900 \cdot 1000 \cdot 400]$.

the shading condition change. Hence, an improved MPPT algorithm has been developed and integrated into the inverter main control. The algorithm can be described in the following two steps. First of all, the algorithm discretely scans the $p-v$ curve with a fixed voltage step extrapolating the reference voltage near to the GMPP. Since the multi peaks, as shown in Fig.4(b) are never too near, the starting voltage point found before it's accurate enough to guarantee that a classical MPPT algorithm, as the well-known P&O algorithm, is able to find the GMPP with accuracy. The output signals from the MPPT algorithm are the v_{dc-ref} and the $Phase$ signal. The $Phase$ signal, which represents the MPPT algorithm status, and the i_{pv} value, are useful to the evaluation of the weighting factor of the FCS-MPC as during the scan phase and with low input current, the dc-voltage reference signal is the most critic one to follow.

IV. Simulation Result

A. Investigated system configuration

In order to verify the control performance, the proposed single-stage grid-connected PV system has been implemented in MATLAB/Simulink and the SimPower Toolbox. The detailed model of a three-level 100-kW grid-connected PV array developed by MathWorks and HydroQuebeck [4] has been taken as based model. The dc boost converter has been removed in order to obtain the single-stage PV system. The SunPower SPR-305E model is used to emulate the PV panel. The PV plant has 4 series-connected modules and 30 parallel strings with a nominal rated power of 100 kW.

The proposed control with the updated MPPT technique has been implemented in the inverter of the based model where the utility grid is connected to a 100kVA-260V/25kV three-phase coupling transformer and it is characterized by 25kV distribution feeder plus a 120kV equivalent transmission system. The parameters of the investigated single-stage PV system are given in Tab. I.

B. Performance in partially shaded condition

To investigate partially shaded condition by providing different solar irradiance, 3 PV panels has been connected as shown in Fig.5. A diode has been connected in parallel with PV panels to maintain the maximum current flow from PV panels. The proposed single-stage PV system and the PI&MPC system are tested under the sudden irradiance changing condition from $[400 \quad 1000 \quad 800]\ \mathrm{w/m^2}$ to $[1000 \quad 700 \quad 900]\ \mathrm{w/m^2}$ at 0.4s. The Ideal $p-v$ curves with these irradiance sets are shown in Fig. 6. From this figure, it can be observed that the maximum

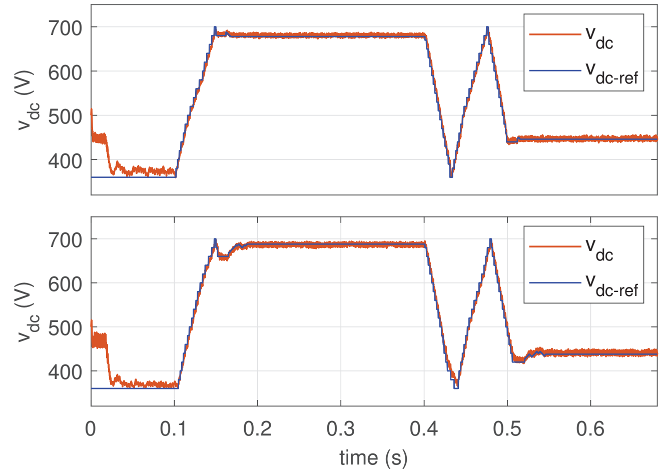

(a)

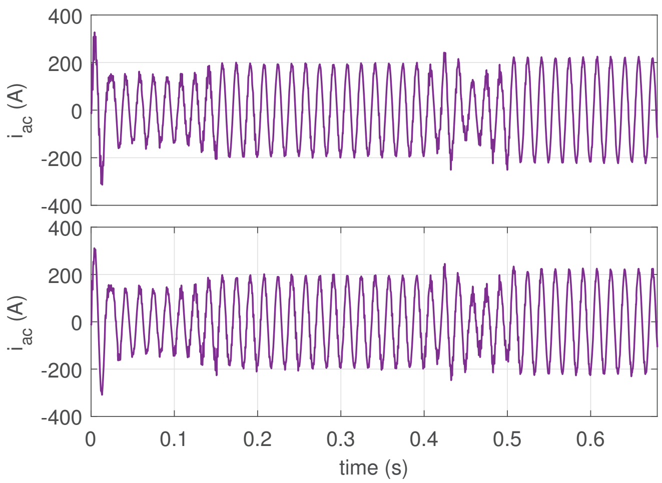

(b)

Fig. 7. Simulation results with the proposed control and the PI&MPC: a)dc-voltage, b)output ac-current in response to a step irradiance change as showed in Fig.6 at 0.4s

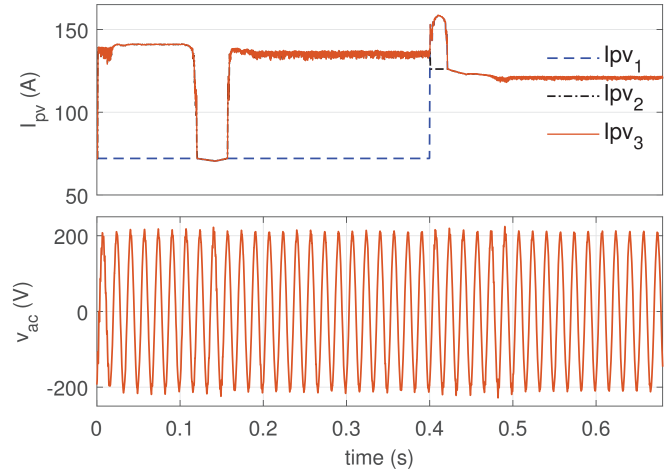

Fig. 8. Simulation results with the proposed control: PV currents and the output ac-voltage in response to a step irradiance change as showed in Fig.6 at 0.4s

powers are 58.8 kW and 67.6 kW with corresponding PV voltages of 684 V and 441.8 V, respectively. A simulation has been carried out for this irradiance change for each system. The events of the simulation are in the following steps: the PV panels are connected since the beginning and at $t = 0.1$ s, the MPPT algorithm is enabled and starts to scan the $p-v$ curve. The simulation results signals: dc voltage and the ac output current are, with the proposed control system and the PI&MPC control are depicted in Fig. 7. With the proposed control, the improved MPPT algorithm can track the MPP within 0.08 s and it's faster compared to the PI&MPC solution in which the v_{dc-ref} calculated from Phase1 of the MPPT algorithm is further from the global MPP due to the fact that the dc-voltage tracking with the PI&MPC is less precisely compare to the proposed solution. The ac-voltage signal with the proposed control shown in Fig.9, is very stable and does not have any impact on the variation of the output power. Instead, the distortion in current i_{ac} in Fig. 7 is related to the distortion from the i_{pv} currents as shown in Fig.8. The same ac voltage and i_{pv} results are obtained with the PI&MPC solution and hence they are not discussed. An important difference between the two compare solutions is the level of THD for the current. The THD at the rated power is 4.5% for the proposed model while it's 5.5% for the PI&MPC control system. Even during the Phase1 of the MPPT algorithm, with the proposed solution less current distortion is obtained.

Furthermore, with the proposed solution, another environmental scenario has been simulated. The proposed single-stage PV system is tested under the sudden irradiance changing condition from $[500 \quad 500 \quad 500]$ $\mathrm{w/m^2}$ to $[900 \quad 1000 \quad 400]$ $\mathrm{w/m^2}$ at 0.4s, in other word, from a uniform irradiance condition to a partially shaded condition. The Ideal $p-v$ curves with these irradiance sets are shown in Fig. 4. From this figure, it can be observed that the maximum powers are 54.2 kW and 53.4 kW with corresponding PV voltages of 650.1 V and 446.7 V, respectively. For these last irradiance profile and the dc-link voltage, ac output current, the i_{pv} currents and the voltage at the PCC are shown in Fig. 9. These last simulations results show the capability of the proposed solution to work under uniform or shaded condition, maintaining stable the output signals through the entire dynamic. The input and output power comparison, with the proposed solution, for each simulated scenario, is presented in Fig.10. At the steady-state, the extracted power for the scenario shown in Fig.6 is equal to 58.1 and 66.6 kW, for the scenario shown in Fig.4 is equal to 53.6 and 52.8 kW, respectively. Each value is very close to the ideal MPP with a general efficiency of 99%.

V. Conclusions

An efficient FCS-MPC control in combination with an improved MPPT strategy is presented for the single-stage grid-tied PV system. The addition of a new constraint to

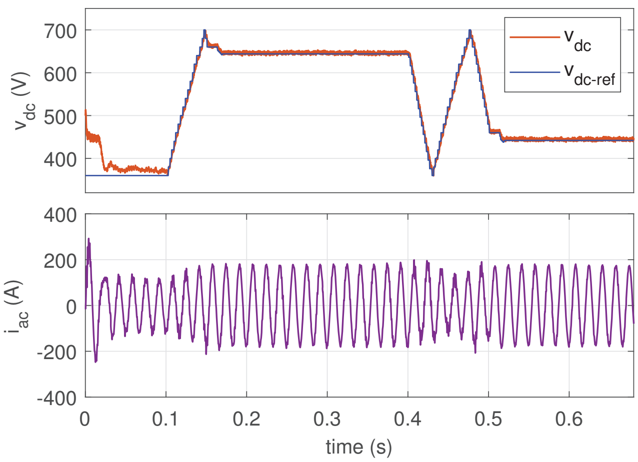

(a)

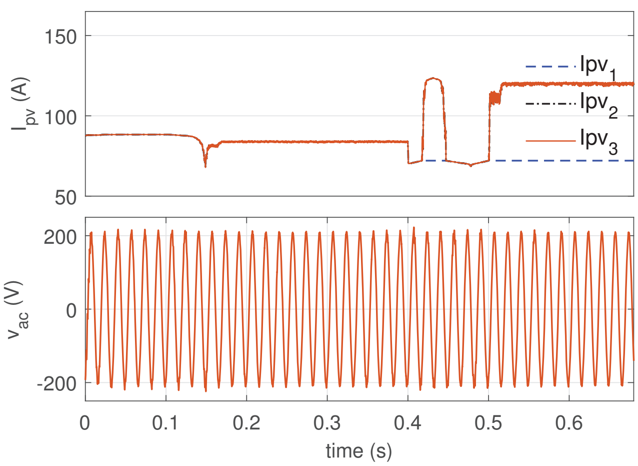

(b)

Fig. 9. Simulation results with the proposed control: a) dc-voltage and output ac current, b) PV currents and output ac voltage in response to a step irradiance change as showed in Fig.4 at 0.4s.

the cost factor equation makes the FCS-MPC more adaptive in tracking the dc-link reference voltage value. Comparative simulation analysis implies the effectiveness of the proposed control technique in tracking the global maximum power point under partially shaded condition. Moreover, the simulation analysis for partially shaded step irradiance change indicates the superiority of the proposed control in making the system work in the entire $p - v$ characteristic, ensuring a stable output signal and the maximum power extraction during all the transient conditions.

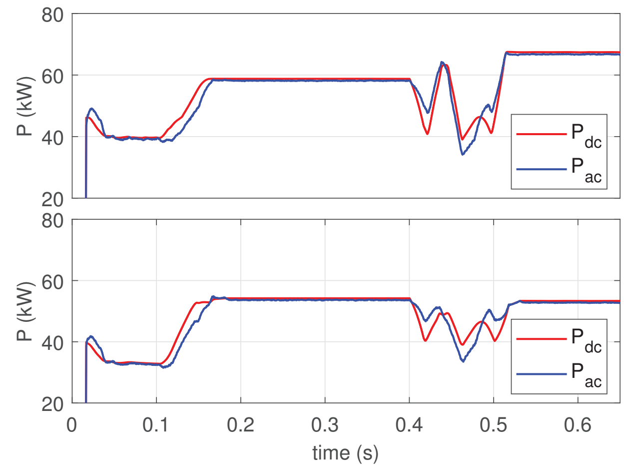

Fig. 10. Output power of the proposed control system in response to a step irradiance change as showed in Fig.6 and Fig.4 respectively at 0.4s

References

[1] "Sertac Bayhan and Haitham Abu-Rub". "40 - predictive control of power electronic converters". In "Muhammad H. Rashid", editor, *"Power Electronics Handbook"*, pages "1325 – 1338". "Butterworth-Heinemann", "fourth edition" edition, "2018".

[2] T. Dragicevic. Model predictive control of power converters for robust and fast operation of ac microgrids. *IEEE Trans. Power Electron.*, 33(7):6304–6317, 2018.

[3] Akel Fethi, Bendib Douadi, Mohammed Laour, and Berkouk El-madjid. Power control of three phase single stage grid connected photovoltaic system. In *2016 International Renewable and Sustainable Energy Conference (IRSEC)*, pages 1136–1141, 2016.

[4] Pierre Giroux, Gilbert Sybille, Carlos Osorio, and Shripad Chandrachood. Detailed model of a 100-kw grid-connected pv array. Accessed 01 Feb 2021.

[5] M. Hamdi, M. Hamouda, L. Sbita, and K. Al-Haddad. Fcs-mpc for grid-tied three-phase three-level npc inverter with experimental validation. In *2017 International Conference on Green Energy Conversion Systems (GECS)*, pages 1–6, 2017.

[6] J. He and Y. W. Li. Generalized closed-loop control schemes with embedded virtual impedances for voltage source converters with lc or lcl filters. *IEEE Trans. Power Electron.*, 27(4):1850–1861, 2012.

[7] Sachin Jain and Vivek Agarwal. Comparison of the performance of maximum power point tracking schemes applied to single-stage grid-connected photovoltaic systems. *IEE Proc. Electric Power Appli.*, 1:753 – 762, 10 2007.

[8] J. Rocabert, A. Luna, F. Blaabjerg, and P. RodrÃguez. Control of power converters in ac microgrids. *IEEE Trans. Power Electron.*, 27(11):4734–4749, 2012.

[9] C. A. Rojas, J. Rodriguez, F. Villarroel, J. R. Espinoza, C. A. Silva, and M. Trincado. Predictive torque and flux control without weighting factors. *IEEE Trans. Ind. Electron.*, 60(2):681–690, 2013.

[10] B. Sahan, A. N. Vergara, N. Henze, A. Engler, and P. Zacharias. A single-stage pv module integrated converter based on a low-power current-source inverter. *IEEE Trans. Ind. Electron.*, 55(7):2602–2609, 2008.

[11] P. Shah, I. Hussain, and B. Singh. Fuzzy logic based fogi-fll algorithm for optimal operation of single-stage three-phase grid interfaced multi-functional secs. *IEEE Trans. Ind. Informat.*, 14(8):3334–3346, 2018.

[12] E. Wu and P.W. Lehn. Digital current control of a voltage source converter with active damping of lcl resonance. In *Twentieth Annual IEEE Applied Power Electron. Conf. and Exposition, 2005.*, volume 3, pages 1642–1649 Vol. 3, 2005.

[13] Z. Zhang, H. Fang, F. Gao, J. RodrÃguez, and R. Kennel. Multiple-vector model predictive power control for grid-tied wind turbine system with enhanced steady-state control performance. *IEEE Trans. Ind. Electron.*, 64(8):6287–6298, 2017.

[14] Y. Zhu, J. Yao, and D. Wu. Comparative study of two stages and single stage topologies for grid-tie photovoltaic generation by pscad/emtdc. In *2011 International Conference on Advanced Power System Automation and Protection*, volume 2, pages 1304–1309, 2011.

[15] YongLi Zhu, JianGuo Yao, and Di Wu. Comparative study of two stages and single stage topologies for grid-tie photovoltaic generation by pscad/emtdc. In *2011 International Conference on Advanced Power System Automation and Protection*, volume 2, pages 1304–1309, 2011.